# Effect of Different Salts on PVAc/PVdF-*co*-HFP Based Polymer Blend Electrolytes

**M. Ulaganathan, S. Rajendran**

*School of Physics, Alagappa University, Karaikudi 630 003, Tamilnadu, India*

Received 15 September 2009; accepted 5 March 2010
DOI 10.1002/app.32404
Published online 24 May 2010 in Wiley InterScience (www.interscience.wiley.com).

**ABSTRACT:** Solid polymer electrolytes comprising poly(vinyl acetate) (PVAc), and poly(vinylidene fluoride-*co*-hexafluoropropylene) (PVdF-*co*-HFP), low molecular weight plasticizer [Ethylene Carbonate (EC)] and different lithium salts ($LiBF_4$, $LiClO_4$, and $LiCF_3SO_3$) are prepared by solution casting technique. The electrolyte films are subjected to various characterization techniques such as XRD, FTIR, DSC, SEM and ac impedance analysis. Ionic conductivity is obtained as a function of frequency at various temperatures ranging from 302 to 363 K. The maximum room temperature ionic conductivity is found to be $1.18 \times 10^{-3}$ S cm$^{-1}$ for the film containing $LiBF_4$ and the temperature dependent ionic conductivity values seem to obey VTF relation. Microstructure of the samples has been depicted by means of scanning electron microscope. © 2010 Wiley Periodicals, Inc. J Appl Polym Sci 118: 646–651, 2010

**Key words:** ethylene carbonate; poly(vinyl acetate); poly(vinylidene fluoride-*co*-hexafluoropropylene); scanning electron microscope; ionic conductivity

## INTRODUCTION

Now a days, polymer electrolytes are promising candidates for the energetic electronic devices, such as lithium battery, super capacitors, chemical sensors, fuel cells, etc.[1,2] Though the polymer electrolytes have many advantages, such as high performance, size, safety, environmental aspects, they still suffer from certain critical drawbacks, which should be overcome before their use in practical applications. Initially, In 1973 Wright and coworkers[3] found the ionic conductivity of PEO and alkaline salt complexes. Unfortunately, due to the particular structure, PEO showed much higher crystalline ratio at room temperature, resulting in a very low room temperature ionic conductivity ($\sim 10^{-7}$ S cm$^{-1}$), which is a drawback for its applications in the consumer electronic market.[4] To date several polymer hosts have been investigated and developed for improving their room temperature ionic conductivity and the mechanical stability, including poly(ethylene oxide) (PEO), poly(acrylonitrile) (PAN), poly(methyl methacrylate) (PMMA), poly(vinyl chloride) (PVC), poly(vinylidene fluoride) (PVdF), poly(vinylidene fluoride-hexafluoro propylene) (PVdF-HFP), poly (ethyl methacrylate) (PEMA), etc.[5–7] Among them (PVdF-HFP) has drawn much attention of researchers because it is a copolymer consisting of crystalline vinylidene fluoride (VdF) and amorphous hexafluoropropylene (HFP) units. It has been known that the PVdF-HFP is very useful as the polymer matrix material in the polymer electrolyte of lithium rechargeable battery, due to its excellent chemical stability mainly supported by VdF unit, as well as due to the enhanced plasticity (somewhat associated with high ionic conductivity) by HFP unit.[8] Further, the room temperature ionic conductivity of the polymer electrolytes can be considerably enhanced by the addition of low molecular weight and high dielectric constant plasticizers such as ethylene carbonate (EC) and propylene carbonate (PC) etc.[9,10]

In general, the solid polymer electrolytes are losing their mechanical strength when the plasticizers are added. The plasticizer added films have to be hardened by either chemical or physical curing, which leads high processing costs. In this study, to prepare films with good mechanical strength and high ionic conductivity, we have chosen a copolymer of vinylidene fluoride and hexafluoropropylene (PVdF-*co*-HFP), the amorphous polymer poly(vinyl acetate) (PVAc), low molecular weight plasticizer and the different lithium salts. The prepared films were subjected to various characterization techniques, such as ac impedance analysis, XRD, FTIR, DSC, and SEM.

## EXPERIMENTAL

All the samples were prepared by solution casting technique.[11] PVAc, PVdF–HFP, and Ethylene Carbonate

*Correspondence to:* M. Ulaganathan (nathanphysics@gmail.com).

**TABLE I**
**Ionic Conductivity of the Complexes at Different Temperatures**

| Sample code | Wt % of compositions of prepared samples [6.25/18.75/67/8 (wt %)] | Conductivity ($\times 10^{-3}$ S cm$^{-1}$) | | | | | | |
|---|---|---|---|---|---|---|---|---|
| | | 302 K | 313 K | 323 K | 333 K | 343 K | 353 K | 363 K |
| E1 | PVAc/PVdF-*co*-HFP/EC/$LiBF_4$ | 1.180 | 1.200 | 1.240 | 1.95 | 2.27 | 2.35 | 2.40 |
| E2 | PVAc/PVdF-*co*-HFP/EC/$LiClO_4$ | 0.398 | 0.449 | 0.491 | 0.528 | 0.667 | 0.733 | 0.800 |
| E3 | PVAc/PVdF-*co*-HFP/EC/$LiCF_3SO_3$ | 0.175 | 0.209 | 0.248 | 0.306 | 0.387 | 0.386 | 0.398 |

(EC) (Aldrich, USA) were used as received. Lithium perchlorate ($LiClO_4$), lithium tetrafluoroborate ($LiBF_4$), and lithium trifluoromethane sulfonate ($LiCF_3SO_3$) were dried by annealing them under vacuum at 120, 70, and 80°C, respectively for 24 h. All components, namely the selected lithium salt (8 wt %) and polymers PVAc (6.25 wt %), PVdF-HFP (18.75 wt %) were dissolved in an anhydrous tetrahydrofuran (THF) and the plasticizer EC (67 wt %) was added to the mixture. The complex was stirred well around 24 h with the help of a magnetic stirrer. Finally the obtained solution was cast on a glass plate and the solvent was allowed to evaporate slowly at room temperature for 48 h. The films were dried in a vacuum oven at 333 K under a pressure of $10^{-3}$ Torr for 24 h. The resulting films were visually examined for their dryness and free standing nature. Chemical storage and film casting were performed under a vacuum. The electrolytes were prepared for different lithium salts as depicted in Table. I.

The ionic conductivity studies were carried out with the help of stainless steel blocking electrodes by using a computer controlled micro auto lab Type III Potentiostat/Galvanostat of frequency range 1 Hz–300 kHz in the temperature range 302–363 K. The structural and complex formations of the electrolytes were confirmed by X-ray diffractometer (*X'*pert PRO PANalytical) using Cu-$K_\alpha$ radiation as source and operated at 20 KV. The sample was scanned in the 2θ ranging from 10–80° for 2 sec in step mode. Fourier transform infra red (FTIR) spectroscopy studies were carried out using SPECTRA RXI, PerkinElmer spectrophotometer in the range 400–4000 cm$^{-1}$. The thermal behavior of the prepared samples was deliberated using a differential scanning calorimeter (DSC) (Mettler Toledo DSC 822e apparatus). The samples were heated from −50 to 300°C at a heating rate of 10°C/m. Surface morphology of the samples was examined by using JEOL, JSM-840A scanning electron microscope (SEM).

## RESULTS AND DISCUSSION

### XRD analysis

XRD pattern of $LiBF_4$,$LiCF_3SO_3$, $LiClO_4$, PVdF-HFP, PVAc polymer, and prepared electrolyte samples are shown in Figure 1(a–h). The characteristic peaks confirm the crystalline nature of the lithium salts as shown in Figure 1(a). In general PVdF-HFP is a semicrystalline polymer and it shows the characteristic peaks at 2θ = 17, 19, and 38°, which correspond well with the (100), (110), and (021) reflections of crystalline phase of PVdF polymer.[12] In Figure 1(e). a single broad peak is found at 2θ = 28°, which confirms the complete amorphous nature of the PVAc polymer. It is observed that crystallinity of solid polymer electrolytes is greatly decreased by the addition of plasticizer and the lithium salts. The characteristic peaks correspond to the lithium salts are not observed in the electrolyte system[Fig. 1(f–h)] indicating that the lithium salts are well complexed in the polymer matrix, which means that the lithium salts do not contain any separate phase in the electrolyte system and it also confirms the complexation.

### FTIR studies

Infrared spectral (IR) analysis is a powerful tool for identifying the nature of bonding and different functional groups present in a sample by monitoring the vibrational energy levels of the molecules, which are essentially the fingerprint of different molecules.[13,14]

Figure 2 depicts the FTIR transmittance spectra in the range 400–4000 cm$^{-1}$ for pure polymers, lithium salts, plasticizer, and their complexes. The vibrational bands observed at 2933 cm$^{-1}$ is assigned to —$CH_3$ asymmetric stretching of PVAc which is shifted to 2943, 2963, and 2967 cm$^{-1}$ in the complexes E1, E2, and E3, respectively. The band at 2465 cm$^{-1}$ is ascribed to —$CH_3$ symmetric stretching vibration of PVAc, which is also shifted to 2494, 2469, and 2489 cm$^{-1}$ in the complexes E1, E2, and E3, respectively. The peaks at 1734, 1033, 1373, and 1243 cm$^{-1}$ are attributed to C=O stretching, C—O stretching, —$CH_3$ symmetric bending and C—O—C symmetric stretching modes of PVAc, which are shifted in the complexes. The peak at 947 cm$^{-1}$ of PVAc corresponding to CH bending vibration is absent in the complexes. The vibrational peak at 609 cm$^{-1}$ is assumed to be linked with $CH_3$ (C—O) group of PVAc and the C—H rocking mode of vibration of PVAc has been confirmed by the presence of a band at 799 cm$^{-1}$.[15,16]

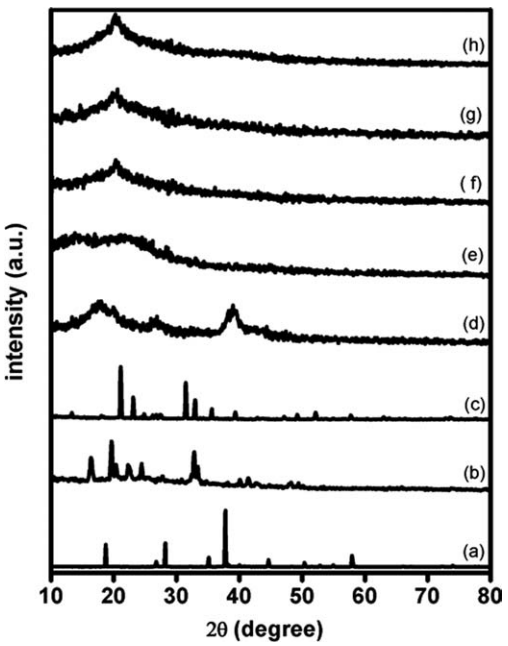


**Figure 1** XRD pattern of Pure (a) $LiBF_4$; (b) $LiClO_4$; (c) $LiCF_3SO_3$; (d) Pure PVdF-HFP; (e) Pure PVAc; (f) PVAc/PVdF-HFP/EC/$LiBF_4$; (g) PVAc/PVdF-HFP/EC/$LiClO_4$; (h) PVAc/PVdF-HFP/EC/$LiCF_3SO_3$;.

The vibrational peaks at 502 and 416 $cm^{-1}$ of PVdF-HFP are assigned to bending and wagging vibrations of $-CF_2$, respectively, which are absent in the complexes. Crystalline phase of the PVdF-HFP polymer is identified by the vibrational bands at 985, 763, and 608 $cm^{-1}$.[17] The strong absorption peak appeared at 1173 $cm^{-1}$ is assigned to the symmetrical stretching mode of $-CF_2$ group which is shifted to 1162, 1171, and 1161 $cm^{-1}$ in the complexes E1, E2, and E3 respectively. The peak appeared at 1390 $cm^{-1}$ is assigned to the $CH_2$ groups of PVdF-HFP,[18–20] which is also shifted to 1369, 1396, and 1401 $cm^{-1}$ in the E1, E2, and E3 complexes.

The peaks at 1770, 1776, and 1775 $cm^{-1}$ corresponding to E1, E2, and E3 are ascribed to the $\nu C{=}O$ (1788 $cm^{-1}$) band of ethylene carbonate. The vibrational peak at 1493 $cm^{-1}$ of pure EC is shifted to 1473, 1479, 1475 in the complexes. Apart from these, some of the peaks appearing at 1597, 1076, 894, and 716 $cm^{-1}$ of EC are absent in the complexes.

The absorption peaks at 2359, 2157, 2027, 1806, and 986 $cm^{-1}$ of PVAc 2984, 2626, 2317, 2203, and 2024 $cm^{-1}$ of PVdF-HFP 2827, 2765, 2554, 2048, 1597, and 974 of ethylene carbonate (EC) are absent in the complexes. It is clear that the band assignments of the complexes are shifted from their pure spectra.

The vibrational peak appeared at 762 $cm^{-1}$ in the spectrum relative to the sample E1 [Fig. 2(g)] is attributed to the vibration mode of free $BF_4^-$ anions and the vibrational mode corresponding to the ion pairs of $BF_4^-$ is appeared at 784 $cm^{-1}$ in the complex system.[21] The FTIR spectrum shows [Fig. 2(h)] the vibrational peaks at 622 and 638 $cm^{-1}$ is corresponding to the anion $ClO_4^-$ and the ion pairs of $ClO_4^-$, respectively.[22] Presence of the band at 768 $cm^{-1}$ in the complex system [Fig. 2(i)] has been attributed to the 'free' triflate anion ($CF_3SO_3^-$).[23] It is noted that the vibrational peak corresponding to the free anion of the salts such as $BF_4^-$, $ClO_4^-$, and $CF_3SO_3^-$ are shifted in the complexes, which confirm the interaction between the polymers and the salt. In addition, some new peaks are present and some of them are absent in the complexes. Thus the spectral analysis confirms the complexation of these two polymers, plasticizer, and lithium salt.

## Ionic conductivity

The electrochemical impedance spectroscopy is an excellent tool to characterize many of the electrical properties of materials and their interfaces with the electronically conducting electrodes. In this study,

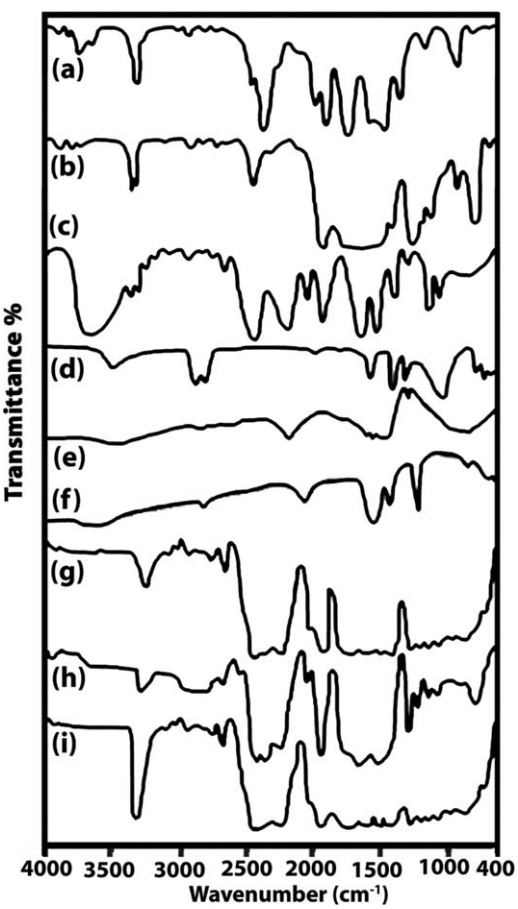


**Figure 2** FTIR spectra of (a)PVAc; (b) PVdF-HFP; (c) EC; (d) $LiBF_4$; (e) $LiClO_4$; (f) $LiCF_3SO_3$; (g) PVAc/PVdF-HFP/EC/$LiBF_4$; (h) PVAc/PVdF-HFP/EC/$LiClO_4$; (i) PVAc/PVdF-HFP/EC/$LiCF_3SO_3$.

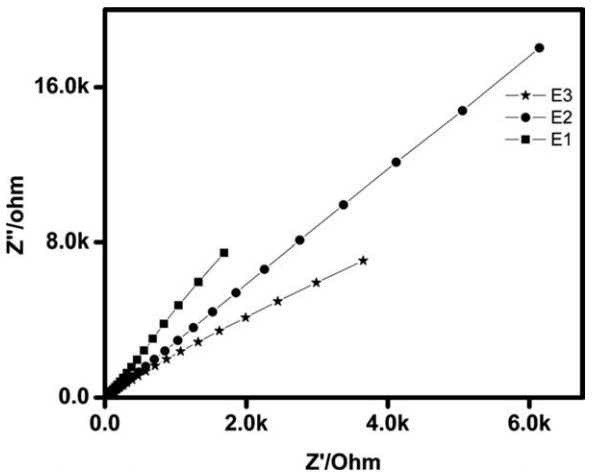


**Figure 3** Complex impedance plot of prepared samples at room temperature.

the ionic conductivities of PVAc/PVdF-HFP/EC/LiX complex with different lithium salts have been estimated keeping the blend ratio of polymer and plasticizer as constant. From the complex impedance plot (shown in Fig. 3), at high frequency region, one can expect the semicircular portion, which do not appear and this is due to the maximum measurable frequency not in the measured range of the instrument. Nevertheless, as the intercept on the $Z'$ (real axis) was clearly noted, we took the intercept values for the samples bulk resistance ($R_b$). A spike (at lower frequency region) corresponds to interfacial impedance of the electrodes. The ionic conductivity of the solid polymer electrolytes was calculated using the equation $\sigma = l/R_bA$, where $\sigma$ is the ionic conductivity, $l$ the thickness of the polymer electrolyte film, $A$ the surface area of the film, and $R_b$ the bulk resistance. The temperature dependent ionic conductivity values of the samples have been given in Table. I. It is also concluded from Figure 4. that the ionic conductivity values of the samples seem to obey VTF relation namely $\sigma = AT^{-1/2} \exp(-B/K(T - T_o))$ where $A$, $B$ are constants and $T_o$ the temperature at which conductance tends to zero and this equation describes the transport properties in a viscous matrix.[24]

The temperature dependence of the ionic conductivity of the films containing different lithium salts $LiBF_4$, $LiCF_3SO_3$, $LiClO_4$, is shown in Figure 4. From the plot of log$\sigma$ *Vs* inverse of temperature ($T$), it is understood that PVAc (6.25)/PVdF-HFP (18.75)/EC (67) LiBF4 (8) film exhibits higher conductivity of the order of $1.18 \times 10^{-3}$ S cm$^{-1}$ at 302 K. The difference in the ionic conductivity is due to the difference in the lattice energies of the various lithium salts. Among the lithium salts, $LiBF_4$ has the lowest lattice energy (699 KJ/mol) and therefore easier solvation of $Li^+$ ion by the polymer matrix, which facilitates for higher ionic conductivity of the sample E1. A similar observation has been reported by Manuel et al.[25,26] Choi et al.[22] reported the ionic conductivity value $2.3 \times 10^{-3}$ S cm$^{-1}$ at 298K for the system PVAc/PVdF-HFP with $LiClO_4$ employing double plasticizer (EC, PC). From the plot (Fig. 4) it is observed that as the temperature increases the ionic conductivity also increases for all the polymer electrolytes, which can be rationalized by the free volume model.[27] As the temperature increases, the polymer can expand easily and produce free volume. Thus ions, solvated molecules, or polymer segments can move into the free volume. The resulting conductivity represented by the overall mobility of ion and polymer is determined by the free volume around the polymer chains. Therefore, as the temperature increases, the free volume increases. This leads to an increase in ion mobility and segmental mobility that will assist ion transport and virtually compensate for the retarding effect of ion clouds.[28] The nonlinearity in Arrhenius plots indicates that the ionic conductivity in polymer electrolyte mainly depends on the polymer chain segmental motion. The ionic conductivity is closely coupled to the segmental motions of the polymer chains and local flexibility i.e. in the electrolytes the ions are coordinated to a macromolecule. It can translate within the system only in conjunction with the segmental motion of the polymer chain. It seems useful to consider the behavior of macromolecular species in which ions are irreversibly bound to a polymer chain i.e., the monomers are surrounded by the ion cloud. Thus the cluster formation is shown to occur when group of interacting polymer segments move from a random distribution throughout the system. It is noted that the given amount of the salt concentrations is

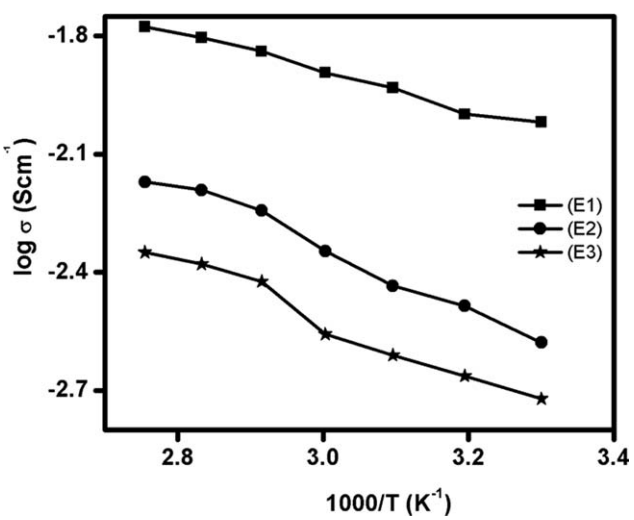


**Figure 4** Temperature dependent ionic conductivity of (a) PVAc/PVdF-HFP/EC/$LiBF_4$; (b) PVAc/PVdF-HFP/EC/$LiClO_4$; (c) PVAc/PVF-HFP/EC/$LiCF_3SO_3$.

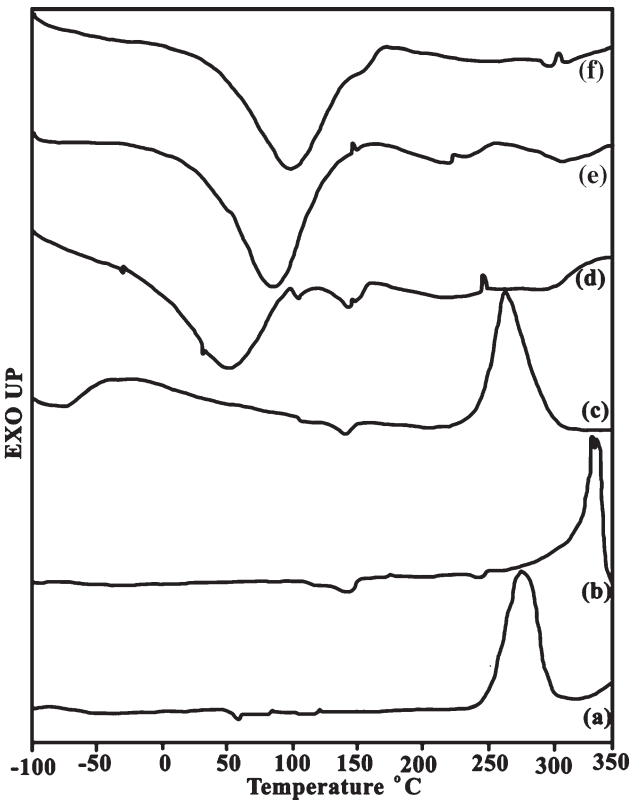


**Figure 5** DSC thermograms of (a) PVAC-$LiClO_4$; (b) PVdF-HFP-$LiClO_4$; (c) PVAc/PVdF-HFP/$LiClO_4$; (d) PVAc/PVdF-HFP/EC/$LiBF_4$; (e) PVAc/PVdF-HFP/EC/$LiClO_4$; (f) PVAc/PVF-HFP/EC/$LiCF_3SO_3$.

superimposed with the free polymer chains or segments which were nearest neighbors to lithium salt ion pair. The plasticizer EC having high dielectric constant would dissolve enough charge carriers and provide more mobile medium for the ions so as to enhance the conductivity behavior of the resultant samples.[29]

## DSC analysis

Figure 5(a–f) shows the DSC thermograms of PVAc+$LiClO_4$, PVdF-HFP+$LiClO_4$, PVAc+PVdF-HFP+$LiClO_4$, PVAc+PVdF-HFP+EC+X ($LiBF_4$, $LiClO_4$, $LiCF_3SO_3$) complex. PVAc+$LiClO_4$ complex has two peaks at 52 and 280°C, which correspond to the transition from glassy phase to rubbery phase ($T_g$) and melting temperature of the complex ($T_m$), respectively. From the thermogram, it is clearly noted that the complex starts to melt around 240°C [Fig. 5(a)]. In fact, it is difficult to determine the glass transition temperature of the PVdF-HFP polymer because of its semicrystalline nature. DSC curve shows [Fig. 5(b)] a single endothermic peak at 142°C, which is attributed to the melting point of PVdF-HFP polymer.[30] Thermogram of the complex PVAc+PVdF-HFP+$LiClO_4$ shows [Fig. 5(c)] endothermic transitions at 100 and 141°C, which correspond to the transition temperature and melting of PVdF-HFP polymer respectively. The thermogram of the complexes E1, E2, and E3 [Fig. 5(d–f)] shows transition peaks at around at 72, 93, and 97°C, respectively. Normally, the addition of plasticizer in the complex changes the thermal behavior of the system. The films E1, E2, and E3 exhibit lower transition temperature compared to PVAc+PVdF-HFP+$LiClO_4$ system, which is mainly due to the addition of Ethylene Carbonate. It is concluded that the addition of plasticizer greatly increased the flexibility of the samples. It is found that the lower transition temperature enhances the ionic conductivity of the complex system.[31] It is noted that the changes in the first order transition temperature with different lithium salts in the complex lead to changes in the ionic conductivity. The complexes E1, E2, and E3 exhibit a second order transition at 220, 202, and 259°C, which correspond to the melting of the complexes.

## SEM analysis

Scanning electron microscope is very useful in studying the morphology of almost all kinds of samples. The morphology of a polymer electrolyte film surface is an important property to characterize the polymer electrolyte.

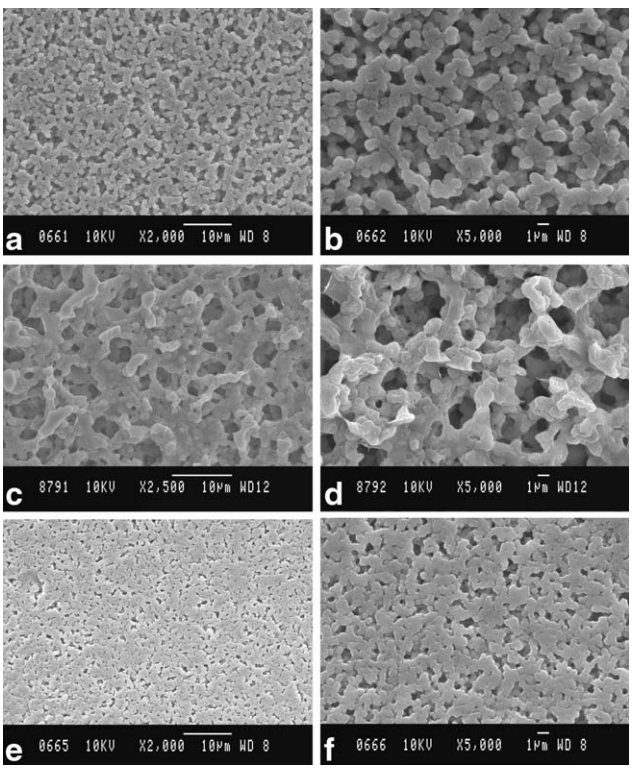


**Figure 6** SEM image of (a) PVAc/PVdF-HFP/EC/$LiBF_4$(2Kx); (b) PVAc/PVdF-HFP/EC/$LiBF_4$(5Kx); (c) PVAc/PVdF-HFP/EC/$LiClO_4$(2.5Kx); (d) PVAc/PVdF-HFP/EC/$LiClO_4$(5Kx); (e) PVAc/PVF-HFP/EC/$LiCF_3SO_3$ (2Kx); (f) PVAc/PVF-HFP/EC/$LiCF_3SO_3$ (5Kx).

Scanning electron microscope (SEM) images of PVAc/PVdF-HFP/EC-LiX ($BF_4$,$CF_3SO_3$,$ClO_4$) based polymer electrolyte films are shown in Figure 6(a–f) at two different magnifications via X2000 and X5000. Figure 6(a,b) shows the photograph of $LiBF_4$ based polymer electrolyte. It is clearly observed from the figure that the spherical segmental grains are mainly due to the host polymer PVdF-HFP and the segmental grains are uniformly distributed in the complex matrix. It contains maximum number of pores and the pore size is (dark region) in the order of 1–10 μm. Figure 6(e,f) reveals the SEM image of $LiCF_3SO_3$ based polymer electrolyte. The surface morphology is smoothed and the segmental grains are lightly disturbed by the plasticizer (EC). The complex has minimum number of pores and their sizes are too small in the order of few hundred nanometers. This may be due to the presence of plasticizer and it reduces the hoping conduction of the sample. The Figure 6(c,d) shows the uniform morphology of $LiClO_4$ based polymer electrolyte. The pores are uniform and their sizes can also be measured from the photograph. The pore morphology of the polymer electrolyte is determined by the solvent nature and evaporation velocity. The evaporation of the solvent is responsible for the creation of the micropores. The ion transport may due to hoping motion with the help of micropores and hence, it enhances the conductivity. It is noted that there is no apparent interface between the two polymers, which indicates that PVAc and PVdF-HFP have good compatibility. From the photograph it is observed that there is no phase separation, which means that the plasticizer does not contain any separate phase; it also indicates that the polymer blend is very compatible with the plasticizer. The presence of pores in microstructures is due to the solvent evaporations because the blended polymer electrolyte has higher solvent retention ability.[32,33] At higher magnification all the samples show the same nature and the effect of plasticizer is also depicted clearly.

## CONCLUSIONS

1. Three different electrolyte systems consisting of PVAc/PVdF-HFP/EC-LiX [X = $BF_4^-$, $ClO_4^-$, $CF_3SO_3^-$] have been prepared using solvent casting technique. The complex formation of the electrolytes has been confirmed from FTIR and XRD studies. Melting temperature of the electrolytes has also been ascertained with the help of differential scanning calorimetry.
2. The maximum ionic conductivity of the polymer electrolyte PVAc/PVdF-HFP/EC-$LiBF_4$ is found to be $1.18 \times 10^{-3}$ S $cm^{-1}$ at 302 K. Hence the properties of PVAc/PVdF-HFP/EC-$LiBF_4$ polymer electrolyte look very desirable and promising for lithium battery applications.
3. The surface morphology of the polymer electrolytes has been studied and the presences of the pores are identified using scanning electron microscope.

## References


1. Song, J. Y.; Wang, Y. Y.; Wan, C. C. J Power Sources 1999, 77, 183.
2. Gnanakumar, G.; Kim, P.; Nahm, K. S.; Elizabeth, R. N. J Membr Sci 2007, 303, 126.
3. Fenton, D. E.; Parker, J. M.; Wright, P. V. Polymer 1973, 14, 589.
4. Croce, F.; Appetecchi, G. B.; Persi, L.; Scrosati, B. Nature 1998, 394, 456.
5. Stephan, A. M. Eur Polym J 2006, 42, 21.
6. Stephan, A. M.; Nahm, K. S. Polymer 2006, 47, 5952.
7. Han, H. S.; Kang, H. R.; Kim, S. W.; Kim, H. T. J Power Sources 2002, 112, 461.
8. Kima, K. M.; Park, N. G.; Ryua, K. S.; Changa, S. H. Electrochim Acta 2006, 51, 5636.
9. Lee, K. H.; Lee, Y. G.; Park, J. K.; Seung, D. Y. Solid State Ionics 2000, 133, 257.
10. Rajendran, S.; Sivakumar, M.; Subadevi, R. Matt Lett 2004, 58, 641.
11. Stephan, A. M.; Gopu Kumar, S.; Renganathan, N. G.; Anbu Kulandainathan, M. Eur Poly J 2005, 41, 15.
12. Abbrent, S.; Plestil, J.; Hlavata, D.; Lingren, J.; Tegenfeldt, J.; Wendsjo, A. Polymer 2001, 42, 1407.
13. Nagatomo, T.; Ichikawa, C.; Omoto, O. J Electrochem Soc 1987, 134, 305.
14. Nagamoto, T.; Kakehata, H.; Ichikawa, C.; Omoto, O. Jpn J Appl Phys 1985, 24, 305.
15. Baskaran, R.; Selvasekarapandian, S.; Hirankumar, G.; Bhuvaneswari, M. S. J Power Sources 2004, 134, 235.
16. Baskaran, R.; Selvasekarapandian, S.; Kuwata, N.; Kawamura, J.; Hattori, T. Mater Chem Phys 2006, 98, 55.
17. Rajendran, S.; Mahendran, O.; Mahalingam, T. Eur Polym J 2002, 38, 49.
18. Rajendran, S.; Mahendran, O.; Kannan, R. Mater Chem Phys 2002, 74, 52.
19. Missan, H. P. S.; Chu, P. P.; Sekhon, S. S. J Power Sources 2006, 158, 1472.
20. Li, Z.; Su, G.; Wang, X.; Gao, D. Solid State Ionics 2005, 176, 1903.
21. Jacob, M. M. E.; Arof, A. K. Electrochim Acta 2000, 45, 1701.
22. Choi, N. S.; Lee, Y. G.; Park, J. K.; Ko, J. M. Electrochim Acta 2001, 46, 1581.
23. Chintapalli, S.; Frech, R. Electrochim Acta 1997, 43, 1395.
24. Capiglia, C.; Saito, Y.; Yamamoto, H.; Mustarelli, P. Electrochim Acta 2000, 45, 1341.
25. Manuel, S. A.; Karan, R. T.; Renganathan, N. G.; Pitchumani, S.; Muniyandi, N.; Ramamoorthy, P. J Power Sources 1999, 81, 752.
26. Manuel, S. A.; Kumar, T. P.; Karan, R. T.; Renganathan, N. G.; Pitchumani, S.; Shrisudersan, J. Solid State Ionics 2000, 130, 123.
27. Miyamoto, T.; Shibayana, K. J Appl Phys 1973, 44, 5372.
28. Ratner, M. A.; Shriver, D. F. Chem Rev 1988, 88, 109.
29. Manuel, S. A.; Kumar, T. P.; Karan, R. T.; Renganathan, N. G.; Pitchumani, S.; Muniyandi, N. J Power Sources 2000, 83, 80.
30. Jiang, Y.-X.; Chen, Z.-F.; Zhuang, Q.-C.; Xu, J.-M.; Dong, Q.-F.; Huang, L. S.; Sun, S.-G. J Power Sources 2006, 160, 1320.
31. Choi, B. K.; Shin, K. H.; Kim, Y. W. Solid State Ionics 1998, 113, 123.
32. Kim, C. S.; Og, S. M. Electrochim Acta 2001, 46, 323.
33. Manuel, S. A.; Saito, Y. Solid State ionics 2001, 148, 475.